A photoluminescence study of poly(phenylene vinylene) derivatives: The effect of intrinsic persistence length

C. L. Gettinger and A. J. Heeger
Institute for Polymers and Organic Solids, University of California, Santa Barbara, Santa Barbara, California 93106

J. M. Drake and D. J. Pine
Exxon Research and Engineering Company, Annandale, New Jersey 08801

(Received 10 January 1994; accepted 7 April 1994)

We report the results of light scattering, absorption, excitation, and emission spectroscopy of three polyphenylene vinylene (PPV) derivatives; poly[2-methoxy, 5-(2′-ethyl-hexyloxy-*p*-phenylene-vinylene] (MEH-PPV), poly[2-butoxy, 5-(2′-ethyl-hexyloxy-*p*-phenylene-vinylene] (BEH-PPV), and poly[2-dicholestanoxy-*p*-phenylene-vinylene] (BCHA-PPV) in solution with *p*-xylene. We find that increasing the size of the solubilizing side chains increases the intrinsic persistence length of the polyphenylene vinylene backbone and that this change in stiffness has dramatic effects on the photoluminescence of polyphenylene vinylene. We have determined the luminescence quantum efficiencies of the polyphenylene vinylene derivatives relative to a known standard, Rhodamine 6G, and find that the photoluminescence can be greatly enhanced by increasing the intrinsic stiffness of the polymer backbone. The stiffest polymer, poly[2-dicholestanoxy-*p*-phenylene-vinylene] (BCHA-PPV), has a quantum efficiency of 0.66 ± 0.05. The quantum efficiency decreases to 0.22 ± 0.05 for poly[2-butoxy, 5-(2′-ethyl-hexyloxy-*p*-phenylene-vinylene] (BEH-PPV) and 0.20 ± 0.05 for poly[2-methoxy, 5-(2′-ethyl-hexyloxy-*p*-phenylene-vinylene] (MEH-PPV), the most coiled derivative. Excitation profiles of the three derivatives also show an increase in nonradiative decay at high energies when the polymer assumes a more coiled comformation. Thus, the quantum yields are dependent on pump energy.

I. INTRODUCTION

Conducting polymers are a class of materials which combine the electrical and optical properties of traditional semiconductors with the mechanical and processing advantages of polymers. In order to process these materials into films and fibers, they must be put in liquid form, either by melting or by dissolving in volatile solvents which can later be removed by evaporation. Because of their large dielectric constants, however, conjugated polymers in their unfunctionalized form are generally insoluble in most organic solvents which have relatively small dielectric constants (~1–10). Moreover, conjugated polymers frequently decompose before they melt. This intractability has been addressed by adding side chains to the polymer backbone; this reduces the melting point of the polymers and renders them soluble in organic solvents such as chloroform and xylene, by providing an organic layer which surrounds the backbone, much like a surfactant, and renders the polymer more compatible with organic solvents. This technique has been exploited in the processing of important conjugated polymer systems like poly(3-alkylthiophenes) and poly(phenylene vinylenes) (PPV).

Although many conducting polymers are processed in the functionalized form, very little is understood about the effects of functionalization on the electronic, optical, and solution properties of these polymers. Several theoretical studies have addressed the factors which determine the conformation of conjugated polymers in solution.[1–4] The conformation of conducting polymers in solution is determined by the usual entropic and elastic character of the polymer chain and by solvent interactions that occur in saturated polymers. In addition, delocalization of the conduction electrons in conjugated polymer systems and steric effects of the side chains serve to extend the polymer chain. Which of these effects is most important in determining the chain stiffness is still unresolved.

Aime[2] has performed light scattering measurements on two saturated polymers, poly-octene and poly-decene, functionalized with different length side chains. That experiment showed that the steric effects of side chains induce significant expansion of the polymer coils. The strong role that steric effects play in the comformation of conjugated polymers is confirmed by numerical simulations of polydiacetylene[5] and in experimental studies of the solution properties poly(alkythiophenes).[6–8]

The absorption and photoemission of PPV and PPV derivatives have been studied extensively.[9–12] These studies have concentrated on the effects of macroscopic disorder on conductivity, absorption, time scales of luminescence decay, and quantum yields. Using methods such as tensile drawing and gel processing to induce orientation and improve structural order, these experiments have shown that reduction of disorder produces a dramatic reduction in apparent Stokes shift along with spectral narrowing of both the absorption and emission spectrum. These results have been interpreted as an increase in effective conjugation length, L_{eff}, as a result of increasing chain order. Still to be understood is how the effective conjugation length is derived from intrinsic polymer features.

While intrinsic polymer stiffness can be manipulated by

 0021-9606/94/101(2)/1673/6/$6.00

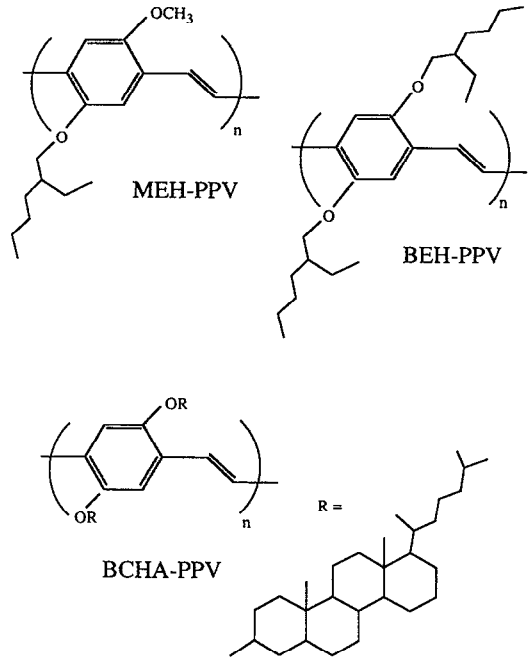

FIG. 1. Poly(phenylenevinylene) derivatives; MEH-PPV, BEH-PPV, BCHA-PPV.

changing the size of the side chains, little is known about how the presence of side chains and the change in stiffness can affect optical and electro-optical properties of these semiconducting polymers. It is these issues which are important to understand when designing polymer derivatives to be used in device applications.

In this paper we report a comparative study of the photoluminescence properties of three PPV derivatives, MEH-PPV, BEH-PPV, and BCHA-PPV (Fig. 1). Each has been functionalized with an increasingly larger side group in order to solubilize the PPV. We have measured the molecular weight M_w and radius of gyration R_g using static light scattering; from these data we infer a persistence length l_p for each PPV derivative. We also measured the hydrodynamic radii R_H using dynamic light scattering. As expected, increasing the size of the side chains increases l_p.

Excitation profile measurements were carried out for the three polymers in solution. The most flexible polymer, MEH-PPV exhibits the largest fraction of nonradiative decay of the photoluminescence; this occurs at energies greater than ~ 3 eV. The fraction of nonradiative decay decreases as the intrinsic stiffness of the polymer is increased. Finally, we determine the luminescence quantum efficiency of the polymers in *p*-xylene relative to quantum yield standard Rhodamine 6G in ethylene gylcol and find that increasing the persistence length of the polymer backbone increases the quantum yield of the system; for BCHA-PPV, the quantum efficiency is 0.66 ± 0.05.

II. EXPERIMENT

HPLC grade *p*-xylene purchased from Aldrich Chemical and was used in all experiments without further purification. The three PPV derivatives, MEH, BEH, and BCHA-PPV were obtained from UNIAX corporation. The synthesis of MEH-PPV and BCHA-PPV have been previously reported.[13]

Static light scattering measurements were performed using a Brookhaven Goniometer and a helium–neon laser ($\lambda = 632.8$ nm) light source. Calibration of the goniometer with toluene showed the system was aligned within $\pm 1\%$ over the angular range $30° \leqslant \theta \leqslant 150°$. Samples used for light scattering measurements were prepared at concentrations below the critical overlap concentration, c^*, filtered through 0.2 μm PTFE filters (Millipore), and centrifuged at low speeds to remove dust in the samples.

The weight average molecular weight M_w, radius of gyration R_g, and the second virial coefficient A_2, were determined in the limit $\theta \to 0$ and $c \to 0$ from the relation[14]

$$\frac{Kc}{R_\theta} = \frac{1}{M_w}\left(1 + \frac{q^2 R_g^2}{3}\right) + 2A_2 c, \tag{1}$$

where $K = 4\pi^2 n^2 (dn/dc)^2 / N_a \lambda_0$ and $q = (4\pi n/\lambda_0)\sin(\theta/2)$ is the scattering wave vector. In the above expressions R_θ is the excess Rayleigh ratio, c is the polymer concentration in g/mℓ, n is the index of refraction of the solvent, λ_0 is the wavelength of light, and dn/dc is the refractive index increment. Refractive index increments were measured on a Chromatix laser differential refractometer.

Dynamic light scattering (DLS) measurements were performed in a Brookhaven goniometer with an ALV-5000 correlator and a Coherent Krypton laser operating at a wavelength of 647.1 nm. Both wavelengths (647.1 and 632.8 nm) used in this experiment were chosen because none of the polymer samples absorbs light at these wavelengths.

DLS investigates particle diffusion by measuring the temporal fluctuations of the scattered light intensity.[15] Temporal fluctuations are characterized by the temporal autocorrelation function of the scattered intensity,

$$g_2(t) \equiv \langle I(t) I(0) \rangle / \langle I \rangle^2. \tag{2}$$

The intensity autocorrelation function can be related to the electric field autocorrelation function $g_1(t)$ through the Siegert relation,

$$g_2(t) = 1 + \beta |g_1(t)|^2, \tag{3}$$

where β is constant determined by the geometry of the collection optics. If fluctuations are due to molecular diffusion, the electric field correlation function decays exponentially as $g_1(t) = \exp(-\Gamma t)$, where $\Gamma = Dq^2$, D is the diffusion coefficient, and q is the scattering vector. The diffusion coefficient can be related to a hydrodynamic radius, R_H, by the Stokes–Einstein equation $D = kT/6\pi\eta_0 R_H$, where k is Boltzmann's constant, T is the temperature, and η_0 is the solvent viscosity.

DLS data were analyzed using the method of cumulants, which accounts for polydispersity of the samples,

$$L(t) = \left[\frac{1}{|g_1(t)|^2}\right]\left[\frac{\partial |g1(t)|^2}{\partial t}\right] = 2q^2\langle D \rangle - 2q^4 \langle \partial D^2 \rangle t + \cdots, \tag{4}$$

where $\langle \partial D^2 \rangle = \langle D^2 \rangle - \langle D \rangle^2$ is the variance in the z-average diffusion coefficient $\langle D \rangle$.

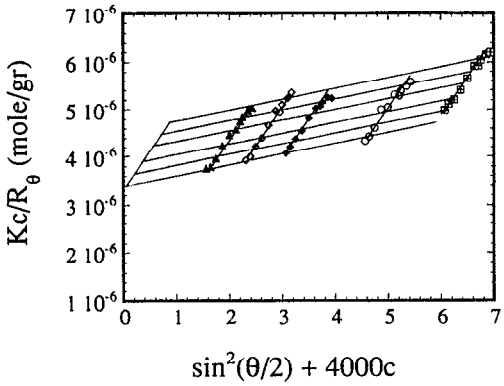

FIG. 2. Zimm plot of BEH-PPV in *p*-xylene.

Absorption spectra were recorded on an IBM Instruments 9420 UV-VIS spectrophotometer.

Excitation and emission spectra were taken on an SLM Aminco 4800S spectrofluorometer. Samples were contained in 1 cm quartz cuvettes and data were collected at right angles from excitation beam.

To minimize reabsorption and re-emission, polymer concentrations ($\sim 10^{-6}$ g/mℓ) were adjusted such that the optical density of all samples were less than 0.1 cm^{-1} at the highest absorption peak. The polarization of the system consisted of the excitation beam at 54.7° and the emission beam vertically polarized. This configuration was chosen to randomize any anisotropy in the excitation and/or emission spectra.

Excitation profiles were obtained by setting the emission monochromater at a specific wavelength and scanning the excitation monochromater. The excitation profiles were normalized to a Rhodamine B quantum counter. In this configuration, the resolution of the excitation and emission monochromater was 1 and 4 nm, respectively.

Emission spectra were taken by setting the excitation monochromater at a specific wavelength and scanning the emission monochromater throughout the visible. The resolution of this configuration was 1 nm for emission and 4 nm for excitation spectra. The emission spectra were corrected for instrumental response.

Quantum yields were determined by comparing the total light emitted from the polymer solutions to the total light emitted from a known standard Rhodamine 6G dissolved in ethylene gylcol.

III. RESULTS AND DISCUSSION

A. Light scattering

The Zimm plot obtained for BEH-PPV is shown in Fig. 2. Similar Zimm plots were also obtained for both MEH-PPV and BCHA-PPV. Extrapolation to zero concentration and zero angle gives values for the molecular weight M_w, degree of polymerization N, and radius of gyration R_g. The results are listed in Table I. Evaluation of the second virial coefficient gives $A_2 \sim 10^{-4}$ for all three polymers and shows

TABLE I. Parameters determined from static and dynamic light scattering.

	MEH-PPV	BEH-PPV	BCHA-PPV
M_w (g/mol)	6.11×10^5	3.06×10^5	9.2×10^5
N	2350	854	1055
A_2 (cm^3 mol/g^2)	1.9×10^{-4}	3.1×10^{-4}	1.1×10^{-4}
R_G (nm)	52.4	42.1	92.1
R_H (nm)	35.9	19.8	33.7
$\rho=R_G/R_H$	1.46	2.13	2.73
l_p (nm)	6.0	11.	40.

that *p*-xylene is a moderate solvent close to theta conditions for all three polymers. In theta solvents, A_2 is ≈ 0.

Intrinsic persistence lengths of the polymers were calculated with the Kratky–Perod model[16] which treats a polymer as a Gaussian distribution of statistical Kuhn lengths. In this model, the radius of gyration, R_g, is expressed as

$$R_G^2 = \frac{n_k b_k^2}{6}, \tag{5}$$

where n_k is the number of Kuhn segments and b_k is the length of the Kuhn segment. The persistence length, l_p, is defined as half a Kuhn length and is explicitly expressed by the relation

$$l_p = \frac{3R_g^2}{L} = \frac{3R_g M_0}{l_0 M}, \tag{6}$$

where L is the contour length of the polymer, M_0 is the monomer molecular weight, l_0 is the monomer length, and M is the molecular weight of the polymer. We have estimated the length of a PPV monomer to be 0.6 nm. Using the values of R_G and M_w obtained from static light scattering, we find that the persistence lengths of the three derivatives are BCHA-PPV 40 nm ($\approx$67 monomer units), BEH-PPV 11 nm ($\approx$18 monomer units), and MEH-PPV 6.0 nm ($\approx$10 monomer units); see Table I. Thus, increasing the size of the side group increases the persistence length of the polymer.

The results of dynamic light scattering measurements are also included in Table I. We obtained concentration-independent hydrodynamic radii for all three polymers in the concentration range studied (10^{-4} g/mℓ), confirming that the polymers are in the dilute limit. We have calculated the overlap concentration c^* to be $\sim 10^{-3}$ g/mℓ for BCHA-PPV the most extended polymer; c^* is even smaller for the other two polymers. Also included in Table I is ρ, which is the ratio of R_g/R_H for the three polymers. This ratio serves as a measure of the stiffness of a polymer and is 1.5 for flexible chains; larger values are indicative of more extended objects.[17] While molecular weight distributions will blur this value, the ratio can be used as a qualitative measure of the comparable stiffness between these polymers. The magnitude of ρ increases from MEH-PPV to BCHA-PPV mirroring the static light scattering results. The values of ρ for these polymers range from 1.46 to 2.76 indicating that while MEH-PPV is a relatively compact coil, BCHA-PPV is a fairly expanded polymer.

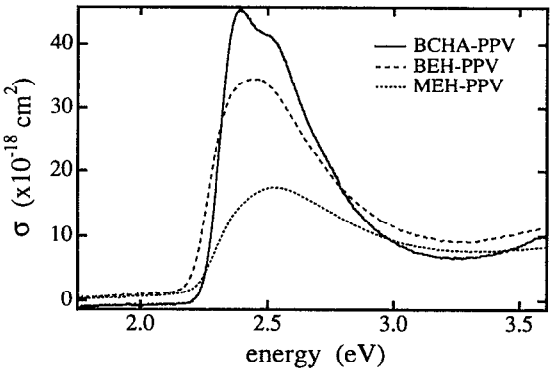

FIG. 3. Absorption spectra expressed in cross section per monomer unit vs photon energy for MEH-PPV, BEH-PPV, and BCHA-PPV in *p*-xylene.

B. Absorption and excitation spectroscopy

The absorption spectra of MEH-PPV, BEH-PPV, and BCHA-PPV in *p*-xylene are shown Fig. 3. The spectra display a flat region at low energies followed by a rapid increase in absorption at ~2.2 eV corresponding to π–π^* electronic transition. The two most flexible polymers, MEH-PPV and BEH-PPV, display the characteristic broadened and featureless spectrum of the absorption transition of conjugated polymers in solution. In contrast, the absorption spectrum of our most rigid sample, BCHA-PPV exhibits two peaks. We attribute the observance of the second peak to an extended resolution of the underlying vibronic structure of the primary electronic transition. As demonstrated by Hagler,[9] this increased resolution directly results from a more ordered structure.

The absorption spectra of solution-cast films of the three polymers have also been measured.[18] For both flexible polymers, MEH-PPV and BEH-PPV, the absorption edge shifts from 2.2 to 2.1 eV going from solution to solid state. This reduction in the band gap is due to an increase in order and is a general feature of conjugated polymers. In contrast, the rigid BCHA-PPV does not show a shift in the band edge going from solution to solid films indicating that this polymer is relatively highly ordered even in solution.

In Fig. 4 the absorption spectra of MEH-PPV, BEH-PPV, and BCHA-PPV are displayed and compared to the excitation profiles of the three polymers measured at 550 nm (2.24 eV). Again, we see a red shift of the peaks of the excitation profiles with increasing stiffness of the polymer mirroring the absorption spectra (see Table II). In these figures, we have plotted the absorption and excitation spectra so that the peaks are at the same height. A striking difference in the three profiles when plotted this way is the much larger absorbance relative to the excitation profile intensity at higher energies in MEH-PPV compared to BCHA-PPV. This indicates that there is a higher probability of nonradiative decay at higher pump energies in MEH-PPV than in BCHA-PPV. This trend also follows the intrinsic stiffness of the polymer. The reduction in the fraction of nonradiative decay for BCHA-PPV implies that the presence of the large, bulky side chains on the PPV backbone not only increases the conjugation length but also appears to suppress an important nonradiative decay mechanism.

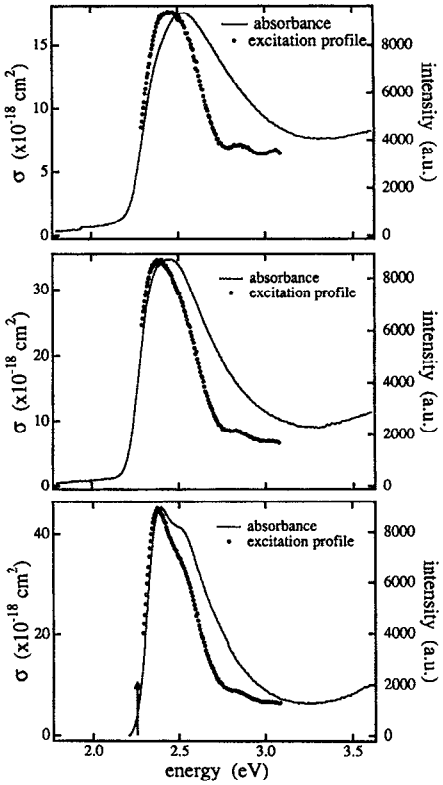

FIG. 4. Excitation spectra (right axis) observed at 550 nm (indicated by vertical arrow) and absorption spectra (left axis) of (a) MEH-PPV; (b) BEH-PPV; (c) BCHA-PPV in *p*-xylene.

Hagler *et al.*[9] have analyzed the absorption spectrum of highly oriented and structurally ordered MEH-PPV as an interband transition with a series of vibrational sidebands. In the most highly ordered samples, the 0→0 transition dominates, with successive sidebands (0→1, 0→2, etc.) having correspondingly smaller contributions as the number of optical phonons involved increases. Disordered samples often show the 0→0 transition weaker with maximum intensity in the 0→1 and 0→2 bands. Comparison with the data in Fig. 4 indicates the following:

(1) BCHA-PPV is a relatively well ordered chain (with correspondingly delocalized electronic wave functions) even in solution.
(2) The nonradiative decay at high pump energies [see Figs. 4(a) and 4(b)] is associated with absorption in vibronic sidebands that involve one or more optical phonons. Fig-

TABLE II. Excitation profile data.

	MEH-PPV	BEH-PPV	BCHA-PPV
Absorption peak (eV)	2.54	2.46	2.40
Excitation peak (eV)	2.44	2.41	2.37

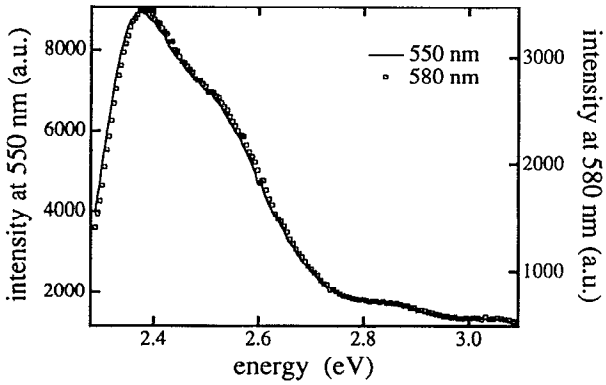

FIG. 5. Excitation profiles of BCHA-PPV observed at 550 and 580 nm.

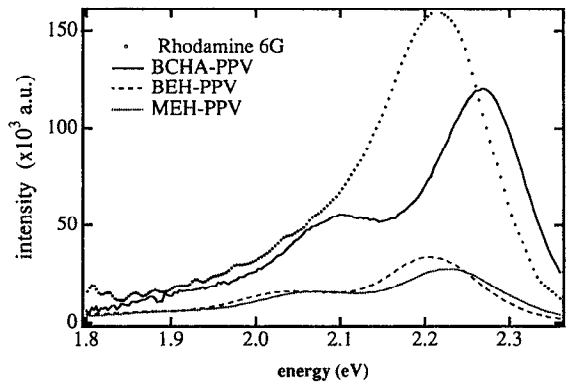

FIG. 6. Photoemission spectra of MEH-PPV, BEH-PPV, BCHA-PPV in *p*-xylene and Rhodaimine 6G in ethylene gylcol.

ure 4(c) (BCHA-PPV) suggests that only the 0→0 transition leads to significant luminescence.

The conclusion that absorption of photons in the vibronic sidebands is inefficient in generating photoluminescense provides an important clue to the origin of the nonradiative decay. Evidently, when the absorption process is not direct (i.e., one or more optical phonons are involved), there is a high probability for multiphonon processes that lead to nonradiative decay. This is qualitatively reasonable; structural relaxation in the excited state is certainly a route to nonradiative decay. The result of Hagler *et al.*[9] indicate that with improved structural order, the Stokes shift decreases and the 0→0 transition dominates; i.e., the system appears to be more nearly harmonic with relatively weak structural relaxation in the excited state. This is consistent with delocalized wave functions in the most highly ordered materials; if the wave functions are delocalized over N carbons, promotion of a single electron in a $\pi \rightarrow \pi^*$ (bonding-anti-bonding) transition will cause a change in the bond charge of only $1/N$. This analysis suggests, therefore, that the achievement of a higher degree of structural order will enhance the probability of radiative photoluminescence decay by suppressing the multiphonon nonradiative channel.

In Fig. 5, we plot the excitation profiles for BCHA-PPV obtained at 550 and 580 nm (2.13 eV). Aside from a difference in absolute intensity, we find these curves to be identical. Excitation profiles obtained for MEH-PPV and BEH-PPV taken at 550 and 590 nm (2.09 eV) are also identical aside from a shift in absolute intensity. These results imply the emission observed at these two energies originates from the same transition. That is, we see no evidence of spectral diffusion at these excitation energies. The scaling for the intensities at the different exciting wavelengths can be calculated from the measured emission spectra; for BCHA-PPV that value was determined to be 2.88. The actual scaling for the excitation profiles measured at 550 and 580 nm was 2.61 roughly a 10% difference. The scaling for BEH-PPV and MEH-PPV also showed a similar 10% difference between the calculated intensity and measured intensity of the excitation profiles.

C. Photoluminescence spectroscopy and quantum efficiencies

In Fig. 6 we show the photoemission spectra of BCHA-PPV, BEH-PPV, and MEH-PPV in *p*-xylene along with Rhodamine 6G in ethylene gylcol. The excitation energy chosen for each polymer corresponds to the energy at which the absorption and excitation curves intersect in Fig. 4. The crossover occurs at 497 nm (2.48 eV) for MEH-PPV, at 512 nm (2.41 eV) for BEH-PPV, and 517 nm (2.39 eV) for BCHA-PPV.

The emission spectra are similar for all three, consisting of a large electronic transition just below the excitation energy followed at lower energies by vibronic progressions which are characteristic of conducting polymers.[9] The apparent Stokes shifts are determined as the energy difference of the peaks of absorption and emission spectra and are summarized in Table III. The Stokes shifts were found to be reduced as the stiffness of the polymer is increased. This reduction in Stokes shifts has also been observed in systems which have been ordered macroscopically via tensile drawing and gel processing.[9]

The quantum yields of our samples in *p*-xylene were measured relative to a standard solution of Rhodamine 6G in

TABLE III. Emission profile data and quantum efficiencies.

	abs. peak (eV)	emiss. peak (eV)	Stokes shift (eV)	QE
MEH-PPV/*p*-xylene	2.54	2.23	0.31	0.20
BEH-PPV/*p*-xylene	2.44	2.20	0.24	0.22
BCHA-PPV/*p*-xylene	2.40	2.28	0.12	0.66
Rhodamine 6G/ethylene glycol	2.32	2.12	0.10	0.95

ethylene gylcol whose absolute quantum efficiency $Q_r \sim 0.94$.[19] The concentration of the standard ($\sim 10^{-6}$) was adjusted so that it had the same optical density as BCHA-PPV. The quantum yield is calculated from the relation[20]

$$Q_x = Q_r \left[\frac{A_r(\lambda_r)}{A_x(\lambda_x)}\right]\left[\frac{I_r(\lambda_r)}{I_x(\lambda_x)}\right]\left(\frac{n_x^2}{n_r^2}\right)\left(\frac{D_x}{D_r}\right). \quad (7)$$

In the above expression $A(\lambda)$ is the absorbance/cm of the solution at the exciting wavelength λ, $I(\lambda)$ is the intensity of the exciting wavelength λ, n is the index of refraction of the solution, and D is the integrated area under the emission spectrum. The subscripts r and x denote the reference sample and the unknown solution. The results are included in Table III. The quantum yield for BCHA-PPV is 0.66 ± 0.05 compared to 0.20 ± 0.05 for MEH-PPV again showing a very strong correlation between intrinsic stiffness and radiative decay in these polymers.

The quantum yield value obtained for MEH-PPV (0.20 ± 0.05) is considerably lower than that obtained by Smilowitz *et al.*[10] Since earlier work utilized DCM as the secondary standard, the overestimate might result from *cis–trans* isomerization of the DCM. Both the isomerization and the resulting effect on the photoluminescence yield are known in the literature.[21]

IV. CONCLUSION

The combined results of absorption, excitation, and emission experiments show a strong correlation between a conjugated polymer's intrinsic rigidity and its optical properties. This correlation is observed in the red shift of the peak absorption, the reduction in Stokes shifts, and increase in quantum efficiencies as the polymer backbone becomes more extended. These results imply that intrinsic chain disorder is reduced when the polymer chains are stiffer. The appearance of vibronic structure in the absorption spectrum of the most rigid derivative, BCHA-PPV is also consistent with the picture of a more ordered structure. It is important to note that a red shift in the absorption spectra, an increase in luminescence, a reduction in Stokes shifts, and a more pronounced vibronic structure is also observed in conjugated systems which have been macroscopically ordered via external methods such as tensile drawing and gel processing. Our results indicate that improved electronic order can be achieved synthetically by using bulkier side groups to enhance chain stiffness. Thus, for some purposes, the extra step of alignment can be removed from the processing of these materials.

The excitation profiles observed at 550 nm of the three derivatives are spectrally similar. The only difference is the shift in peaks towards lower energies as the rigidity is increased. We have also observed the emission at other wavelengths and with the exception of the intensity we find no spectral differences in any of the three polymers at the energies we have observed.

The excitation profiles of these polymers provide important information. Because the profiles *do not* mirror the absorption spectra, emission intensities are dependent upon the wavelength used to excite the polymers. Therefore, reported quantum yields must include this information. The fact that the more rigid structure displays less nonradiative decay is indicative of a suppression of an important nonradiative decay mechanism.

ACKNOWLEDGMENT

This research was partially funded by the National Science Foundation through NSF-DMR-9300366.

[1] J. Aime and F. Bargain, Europhys. Lett. **9**, 35 (1989).
[2] J. Aime, S. Ramakrishnan, R. Chance, and M. Kim, J. Phys. France **51**, 963 (1990).
[3] P. Pincus, G. Rossi, and M. Cates, Europhys. Lett. **4**, 41 (1987).
[4] K. Schweizer, J. Chem. Phys. **85**, 1156 (1986).
[5] J. Bredas and A. Heeger, Macromolecules **23**, 1150 (1990).
[6] G. W. Heffner and D. S. Pearson, Macromolecules **24**, 6295 (1991).
[7] D. R. Spiegel, Macromolecules **23**, 3568 (1990).
[8] J. P. Aime *et al.*, Phys. Rev. Lett. **62**, 55 (1989).
[9] T. W. Hagler, K. Pakbaz, K. F. Voss, and A. J. Heeger, Phys. Rev. B **44**, 8652 (1991).
[10] L. Smilowitz *et al.*, J. Chem. Phys. **98**, 6504 (1993).
[11] H. Bassler *et al.*, Syn. Met. **12**, 49 (1992).
[12] U. Rauscher, H. Bassler, D. D. C. Bradley, and M. Hennecke, Phys. Rev. B **42**, 9830 (1990).
[13] F. Wudl *et al.*, in *Materials for Non-linear Optics: Chemical Perspectives* (American Chemical Society, Washington, D.C., 1991).
[14] M. Huglin, *Light Scattering from Polymer Solutions* (Academic, New York, 1972).
[15] B. Berne and R. Pecora, *Dynamic Light Scattering with Applications to Chemistry, Biology, and Physics* (Wiley, New York, 1976).
[16] O. Kratky and G. Porod, Recl. Trav. Chim. Pays-Bas **68**, 1106 (1949).
[17] H. Kromer *et al.*, Macromolecules **24**, 1950 (1991).
[18] K. Pakbaz (private communication).
[19] M. Lesiecki and J. Drake, Appl. Opt. **21**, 557 (1982).
[20] J. N. Demas and G. Crosby, J. Phys. Chem. **75**, 991 (1971).
[21] J. Drake, M. Lesiecki, and D. Camaioni, Chem. Phys. Lett. **113**, 530 (1985).